Design and Preliminary Characterization of *Ag85B-ESAT-6-Rv2660c* mRNA-Lipid Nanoparticles for TB Vaccine Development

Panadda Dhepakson, Apichai Prachasuphap, Kodcharad Jongpitisub, Pantida Treeyoung, Sirawit Wet-osot, Anicha Luengchaichaweng, Rujiraporn Pitaksalee, and Parnuphan Panyajai

Medical Life Sciences Institute, Department of Medical Sciences, Nonthaburi 11000, Thailand

ABSTRACT Tuberculosis (TB) remains a major global public health challenge, and Thailand is one of the High Burden Country Lists due to its incidence rate exceeding the global average. The only TB vaccine available, Bacillus Calmette–Guérin (BCG), effectively protects against severe TB in children but has limited efficacy in preventing pulmonary TB in adults. Therefore, developing new TB vaccines is crucial to achieving Thailand's goal of TB elimination and sustainable disease control. This study focused on designing and characterizing modified mRNA constructs for a TB vaccine development using three key antigens: Ag85B, ESAT-6, and Rv2660c, which target different stages of *Mycobacterium tuberculosis* (MTB) infection. Five mRNA constructs encoding TB antigens were designed and synthesized *in vitro*, including three single-antigen constructs and two fusion proteins composed of all three antigens. Notably, the fusion mRNA constructs *Ag85B-G4S-ESAT-6-G4S-Rv2660c* mRNA and *Ag85B-AAY-ESAT-6-AAY-Rv2660c* mRNA exhibited greater secondary structure stability compared to single-antigen constructs. Encapsulation of both fusion mRNA constructs in lipid nanoparticles (mRNA-LNPs) demonstrated high encapsulation efficiency, excellent size uniformity (~140 nm), and reliable stability. Moreover, the delivery of mRNA-LNPs into HEK293 cells confirmed the successful expression of fusion proteins for both mRNA constructs, as indicated by TB antigen-specific antibody staining. Therefore, the modified *Ag85B-ESAT-6-Rv2660c* mRNAs exhibited suitable characteristics and significant potential for further development as the tuberculosis vaccine.

Keywords: Tuberculosis, mRNA vaccine, *Ag85B-ESAT-6-Rv2660c*, Lipid nanoparticle

Corresponding author E-mail: panadda.d@dmsc.mail.go.th

Received: 18 March 2025 *Revised: 25 March 2025* *Accepted: 28 March 2025*

Introduction

Tuberculosis (TB), caused by *Mycobacterium tuberculosis* (MTB), remains a major global health challenge.[1] After infection, MTB can persist in a latent state within the human body without causing symptoms, referred to as latent TB infection. However, approximately 5–10% of individuals with latent TB progress to active TB when their immune system is weakened, leading to bacterial proliferation, systemic spread via the lymphatic system, and symptomatic illness.[2]

The Bacillus Calmette–Guérin (BCG) vaccine, developed in 1921 from *Mycobacterium bovis*, is the only TB vaccine available. As a live attenuated vaccine, BCG effectively prevents severe TB in children.[3] However, its efficacy diminishes in adults,[3] highlighting the need for the development of more effective TB vaccines, particularly in high-burden countries like Thailand, which ranks among the top countries globally for TB prevalence.[1] This aligns with Thailand's national strategy to eliminate TB through research and innovation in prevention, treatment, and control measures.[4]

Recent advancements in TB vaccine development have focused on incorporating multiple antigens to target various stages of *M. tuberculosis* infection. Vaccines based on fusion antigens, such as Ag85B-ESAT-6 (H1) and Ag85B-TB10.4 (H4) in protein subunit platforms, as well as Ag85B-ESAT-6 delivered via a DNA platform, have demonstrated enhanced protection in animal models compared to BCG.[5-7] Notably, the multistage subunit vaccine H56, which combines early antigens Ag85B, ESAT-6, and the latency-associated protein Rv2660c, has demonstrated superior protection in animal models. This combination elicits a more comprehensive immune response by targeting both active infection and latent stages of MTB, outperforming Ag85B-ESAT-6 (H1) and BCG in terms of protective efficacy.[8] Further clinical evaluations of the H56:IC31 vaccine in Phase 1b trials have yielded promising results, with no safety concerns observed in adults vaccinated within one month of completing TB treatment. The vaccine successfully induced CD4+ T-cell responses and antibodies specific to the vaccine proteins.[9,10]

While vaccine platforms such as protein subunits and DNA vaccines have shown promise in preclinical and clinical studies, mRNA-based TB vaccines, particularly those incorporating multiple antigens targeting different stages of infection, remain largely unexplored. The potential of mRNA vaccine technology for TB was first demonstrated in 2004 with an mRNA vaccine encoding a single antigen, MPT83, which induced robust humoral and T-cell immune responses in murine models. Although the protective efficacy against MTB infection was lower compared to BCG, this study provided strong evidence that mRNA vaccines could be adapted to improve efficacy by including multiple antigens.[11]

This study aimed to design and characterize modified mRNA constructs for a TB vaccine using three antigens: Ag85B, ESAT-6, and Rv2660c, which targeted different stages of MTB infection. The research included both individual mRNA sequences for each antigen and fusion proteins, *Ag85B-G4S-ESAT-6-G4S-Rv2660c* and *Ag85B-AAY-ESAT-6-AAY-Rv2660c.* These modified mRNA constructs provide a foundation for developing mRNA-based TB vaccines.

Materials and Methods

mRNA Design

The coding sequences for the MTB target antigen genes were designed as the followings: 1) *Ag85B*, 2) *ESAT-6*, 3) *Rv2660c*, 4) *Ag85B-G4S-ESAT-6-G4S-Rv2660c* fusion, and 5) *Ag85B-AAY-ESAT-6-AAY-Rv2660c* fusion. Each sequence was modified by adding the tissue plasminogen activator (tPA) secretory signal and the MHC class I trafficking signal (MITD) to enhance secretion and antigen presentation via MHC molecules. The sequences were optimized using a codon optimization approach, with additional adjustments for uridine depletion, and GC content to ensure efficient translation in human cells[12] using mRNAid software (version 1.0.0) (https://mrnaid.dichlab.org/).[13] The minimum Free Energy (MFE) and the structure of the mRNA were predicted via the RNAfold web server (http://rna.tbi.univie.ac.at/cgi-bin/RNAWebSuite/RNAfold.cgi).

mRNA Synthesis

For template preparation and vector construction, the DNA constructs encoding the MTB antigen genes were synthesized (Gene Universal Inc., USA) and cloned into a linearized template vector (Takara Bio Inc., USA) to serve as a template for *in vitro* transcription. The constructed plasmid DNA (pDNA) was then transformed into *Escherichia coli* (*E. coli*) strain Stbl2 for propagation. Positive clones were identified through colony PCR, using primers specific to all inserts (Forward 5′-AGA GAA CCC GCC ACC ATG-3′, Reverse 5′-CGA GGC TCC AGC TCA TCA-3′). Clones were further confirmed by Sanger sequencing using BigDye™ Terminator v3.1 Cycle Sequencing Kit (Thermo Fisher Scientific, USA) on ABIPRISM® 3500xL Genetic Analyzer (Thermo Fisher Scientific, USA). The verified plasmids were propagated in LB medium at 30 °C for 16 hours (shaken at 225 rpm) and purified using the QIAGEN Plasmid Midi Kit following the manufacturer's protocol. pDNA concentration was determined via absorbance at 260 nm using a NanoDrop™ spectrophotometer (Thermo Fisher Scientific, USA). Plasmids were linearized using the *HindIII* restriction enzyme digestion (16 hours at 37 °C), followed by purification through ethanol precipitation. Complete linearization was confirmed using agarose gel electrophoresis before proceeding to *in vitro* transcription.

For *in vitro* transcription, linearized pDNA served as the template for mRNA synthesis using an IVTpro T7 mRNA Synthesis Kit (Takara Bio Inc., USA). N1-methylpseudouridine-5′-triphosphate was incorporated during synthesis, replacing UTP to enhance stability and reduce immunogenicity. The synthesized mRNA contained essential regulatory elements, including a 5′ untranslated region (UTR), a 3′ UTR, and a poly(A) tail. A co-transcriptional capping strategy was employed using the CleanCap® AG (TriLink Biotechnologies, USA) system, incorporating N7-methyl-3′-O-methyl-guanosine at the 5′ end to ensure efficient and accurate capping. Purification of mRNA was then performed by LiCl precipitation according to the IVTpro T7 mRNA Synthesis Kit protocol. Once purified, mRNA was analyzed using the Agilent TapeStation automated electrophoresis system with RNA ScreenTape (Agilent Technologies, USA) following the manufacturer's protocol and the mRNA Synthesis and Encapsulation in Ionizable Lipid Nanoparticles protocol[14] to assess mRNA integrity, size, and poly(A) tail presence and length.

Encapsulation of mRNA with Lipid Nanoparticles (LNPs)

For the production of mRNA-Moderna-like LNPs, the lipid components used for the preparation of LNPs including 9-heptadecanyl 8-{(2-hydroxyethyl)[6-oxo-6-(undecyloxy) hexyl]amino}octanoate (SM-102) (Cayman Chemical Company, USA), 1,2-distearoyl-sn -glycero-3-phosphocholine (DSPC) (Avanti Polar Lipids, AL, USA), 1,2-dimyristoyl-rac-glycero-3-methoxypolyethylene glycol-2000 (DMG-PEG-2000) (Avanti Polar Lipids, AL, USA), and cholesterol (Sigma, UK). Individual stock solutions of SM-102, DSPC, cholesterol, and DMG-PEG-2000 were prepared by dissolving each lipid component in anhydrous ethanol. These were then combined in a molar ratio of 50:10:38.5:1.5 (SM-102: DSPC: cholesterol: DMG-PEG-2000) to achieve a total lipid concentration of 12.5 mM (1.8 mg/mL). In parallel, mRNA was diluted in a 100 mM acetate buffer (pH 4.0) to achieve a lipid-to-mRNA molar ratio of 4:1 (cationic ionizable lipid: nucleotide). The ethanol-based lipid mixture and the aqueous mRNA solution were then combined using a NanoAssemblr microfluidic device (Precision Nanosystems, Vancouver, BC, Canada) at a 3:1 volume ratio, with a total flow rate of 12 mL/min. The mRNA-LNPs were diluted 40X in PBS and concentrated using an Amicon® Ultra Centrifugal Filter Device with a 10 kDa molecular weight cutoff (Merck Millipore, USA). Finally, the mRNA-LNPs were aliquoted and stored at 4 ˚C until use.[15]

For the production of mRNA-GenVoy-ILM™LNPs (Precision NanoSystems, Vancouver, Canada), GenVoy-ILM™ lipid was purchased from Precision NanoSystems (Vancouver, BC, Canada). A stock lipid solution was prepared by diluting GenVoy-ILM™ in anhydrous ethanol to achieve a total lipid concentration of 12.5 mM. In parallel, mRNA was diluted in a 100 mM acetate buffer (pH 4.0) to achieve a lipid-to-mRNA molar ratio of 4:1 (cationic ionizable lipid: nucleotide). The ethanol-based lipid mixture and the aqueous mRNA solution were then combined using the same Nano Assemblr microfluidic device and processed under identical conditions as the Moderna formulation.

Characterization of the mRNA-LNPs

The hydrodynamic size and polydispersity index (PDI) of the mRNA-LNPs were assessed using dynamic light scattering (DLS) on a Malvern Zetasizer Advance (Malvern Instruments Ltd., Malvern, U.K.). The mRNA-LNPs were diluted 200-fold in PBS before measurement, which was performed at 25°C and a backscattering angle of 173°. The zeta potential of the mRNA-LNPs was measured using the same instrument. Before analysis, concentrated mRNA-LNP stock was diluted 30-fold in sterile PBS (pH 7.4). Measurements were conducted at 25°C using a folded capillary cell (DTS1070).

The % encapsulation efficiency (%EE) of nucleic acid in the LNPs was quantified using the Quant-iT Ribogreen RNA assay kit (Invitrogen, Paisley, Scotland). Briefly, equal concentrations of mRNA-LNPs were prepared with and without treatment by Triton X-100 (Sigma-Aldrich) to lyse the nanoparticles. The samples were incubated for 10 minutes and then transferred to 96-well plates in triplicate, alongside RNA standards. The fluorescent Ribogreen reagent was added according to the manufacturer's instructions, and fluorescence

was measured using a Qubit 4 Fluorometer (Thermo Fisher Scientific, USA). A standard curve was generated to quantify RNA content and %EE was calculated using the following formula:

$$\%EE = \left(\frac{\text{mass of encapsulated mRNA}}{\text{total mass of mRNA detected in the sample}} \right) \times 100\%$$

Transfection and Immunofluorescence Analysis

FreeStyle™ 293-F cells (Thermo Fisher Scientific, USA) were transfected with LNP-formulated mRNA constructs to evaluate functionality. The cells were maintained in FreeStyle™ 293 Expression Medium (Thermo Fisher Scientific, USA) at 37°C with an orbital shaking at 125 rpm in an 8% CO_2 incubator. For transfection, cells were seeded into six-well plates at a density of 2×10^5 cells per well and incubated overnight. The LNP-formulated mRNA was added directly to the cells at 1.0 ug/well. At 72 hours post-transfection, transfection efficiency was assessed by evaluating TB antigen protein expression through immunofluorescence staining. Briefly, cells were harvested, smeared onto slides, and fixed with 4% paraformaldehyde for 15 minutes. Permeabilization was performed using 0.1% Triton X-100. The slides were then incubated with primary antibodies, Rabbit Anti-Ag85B antibody (Abcam, cat. no. ab312328), followed by a secondary incubation with FITC-conjugated Polyclonal Swine Anti-Rabbit Immunoglobulins (DakoCytomation, Denmark). Fluorescence imaging was conducted using a Nikon Eclipse E600 fluorescence microscope (USA) to confirm the expression of TB antigens.

Result

mRNA Design

Five MTB genes; *Ag85B*, *ESAT-6*, *Rv2660c*, *Ag85B-G4S-ESAT-6-G4S-Rv2660c* fusion, and *Ag85B-AAY-ESAT-6-AAY-Rv2660c* fusion were successfully designed for pDNA construction (Figure 1). By optimizing the codons of MTB genes to be suitable for human cells, it was found that the designed genes had a higher codon adaptation index (CAI) value than 0.9, which could enhance protein expression compared to the original genes. Secondary structure analysis of the optimized mRNAs revealed MFE values of -565.1, -296.8, -272.8, -810.7, and -790 kcal/mol for *Ag85B*, *ESAT-6*, *Rv2660c*, *Ag85B-G4S-ESAT-6-G4S-Rv2660c* fusion, and *Ag85B-AAY-ESAT-6-AAY-Rv2660c* fusion, respectively (Figure 2).

MFE values indicate the thermodynamic stability of an mRNA's secondary structure, and a lower (more negative) ΔG indicates a more stable molecule with reduced structural fluctuations.[16] The fusion constructs showed lower MFE values than their components, with MFE values of -810.7 and -790.0 kcal/mol for *Ag85B-G4S-ESAT-6-G4S-Rv2660c* mRNA and *Ag85B-AAY-ESAT-6-AAY-Rv2660c* mRNA, suggesting that these constructs adopt more stable secondary structures. This increased stability reduces susceptibility to mRNA degradation and enhances translational efficiency.

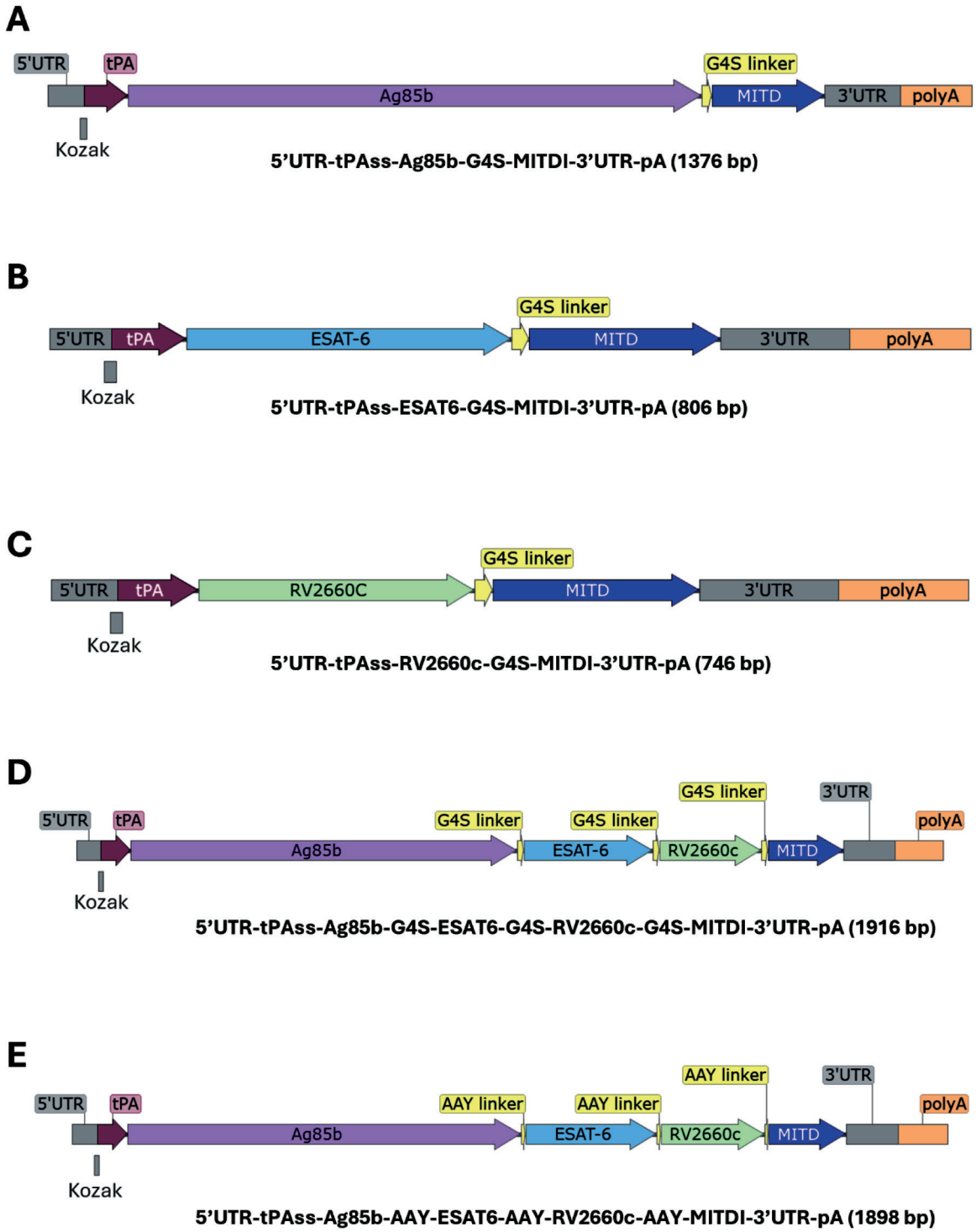

Figure 1 Schematic representation of the five MTB genes used for pDNA construction and subsequent mRNA synthesis via *in vitro* transcription: (A) *Ag85B*, (B) *ESAT-6*, (C) *Rv2660c*, (D) *Ag85B-G4S-ESAT-6-G4S-Rv2660c* fusion, and (E) *Ag85B-AAY-ESAT-6-AAY-Rv2660c* fusion.

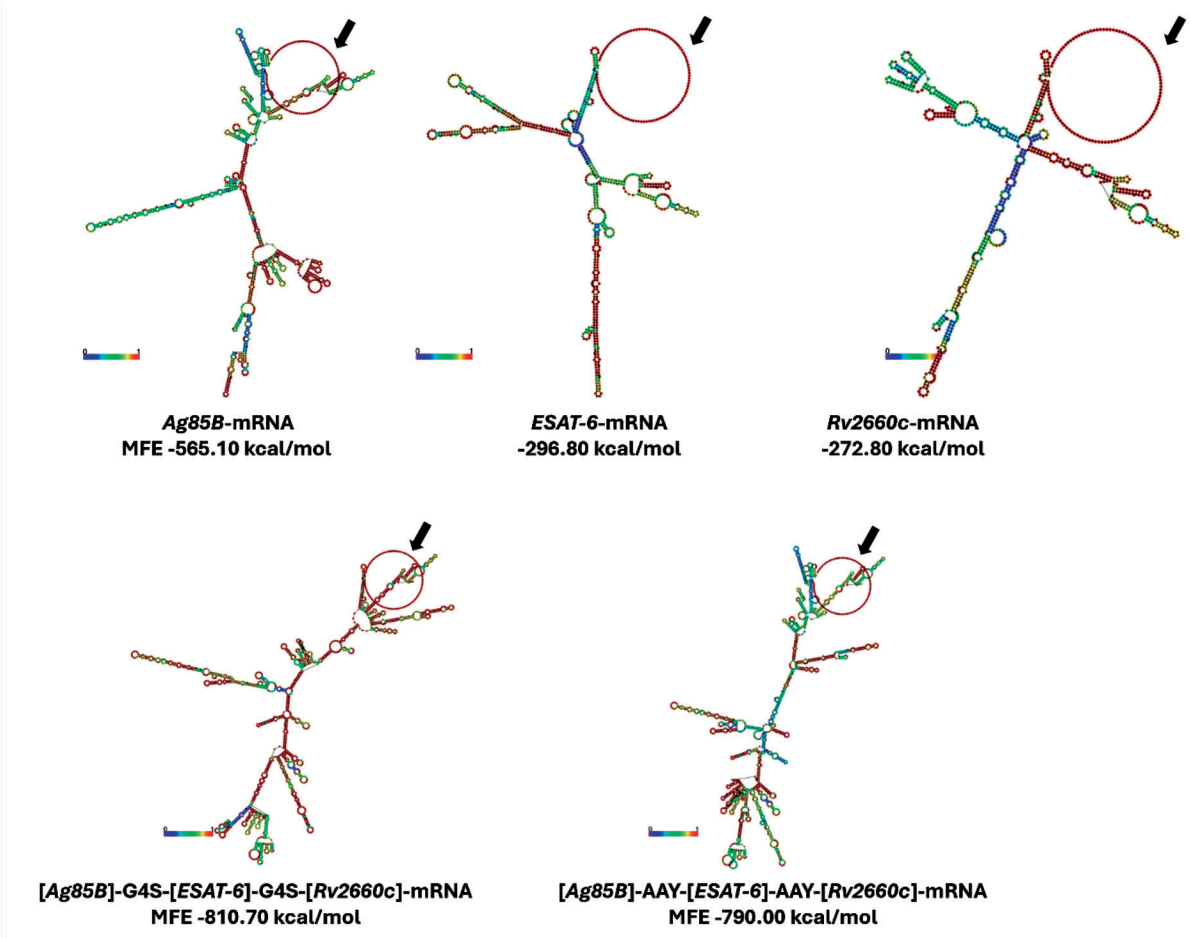

Figure 2 Predicted secondary structures of codon-optimized mRNA generated using the RNAfold web server. The structures are color-coded based on base-pairing probabilities, where red indicates highly unpaired regions (low pairing probability) and blue represents highly paired regions (high pairing probability). Secondary structures such as hairpins and stem-loop structures are shown. The poly(A) tail at the 3′ end of the mRNA is indicated with a black arrow.

mRNA Synthesis

The five MTB genes were successfully cloned into pDNA vectors, verified via colony PCR (Figure 3), and confirmed through Sanger sequencing. Positive clones were expanded in cultures, and pDNA was isolated and linearized using the *HindIII* restriction enzyme (Figure 4). These linearized constructs served as templates for *in vitro* transcription. The transcription reactions successfully generated mRNAs, which were analyzed using an automated gel electrophoresis system (Agilent TapeStation Automated Electrophoresis System with RNA ScreenTape Kit) to assess their molecular size and integrity. The results confirmed that the synthesized mRNAs, including their poly(A) tails, corresponded to the expected sizes for all five genes: 1376 bp (*Ag85B*), 806 bp (*ESAT-6*), 746 bp (*Rv2660c*), 1916 bp (*Ag85B-G4S-ESAT-6-G4S-Rv2660c fusion*), and 1898 bp (*Ag85B-AAY-ESAT-6-AAY-Rv2660c* fusion) (Figure 5). The synthesized mRNAs were intact, with no detectable fragmented mRNAs.

Among the synthesized mRNAs, the fusion constructs *Ag85B-G4S-ESAT-6-G4S-Rv2660c* and *Ag85B-AAY-ESAT-6-AAY-Rv2660c* were selected for encapsulation into LNPs due to their superior MFE values, indicating higher structural stability and translational efficiency.

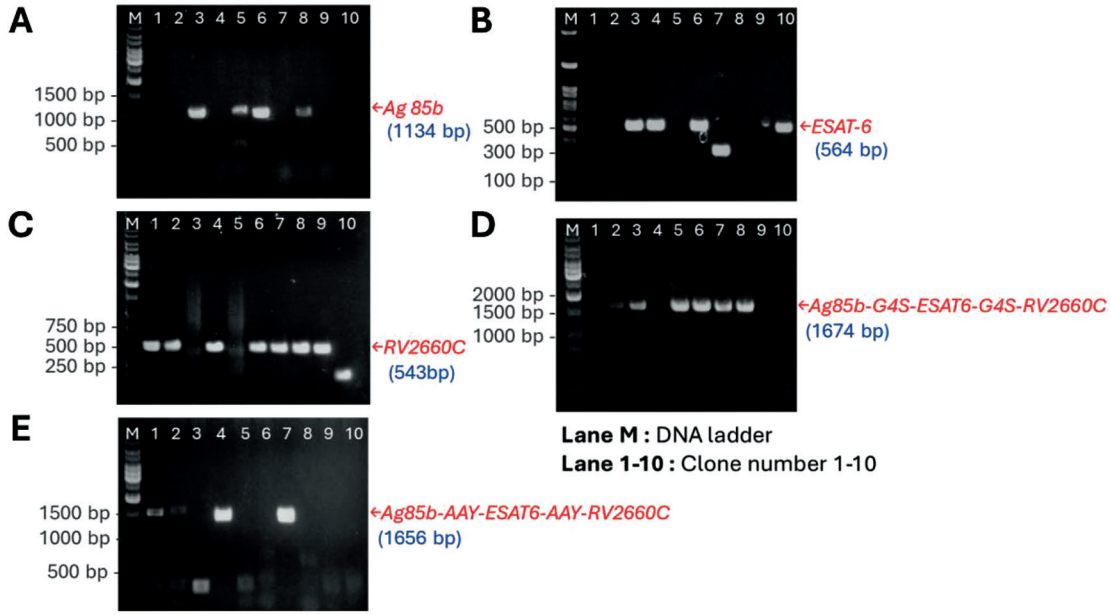

Figure 3 Colony PCR results confirming recombinant pDNA clones in *E. coli* Stbl2 for the five MTB genes: (A) *Ag85B*, (B) *ESAT-6*, (C) *Rv2660c*, (D) *Ag85B-G4S-ESAT-6-G4S-Rv2660c* fusion, and (E) *Ag85B-AAY-ESAT-6-AAY-Rv2660c* fusion.

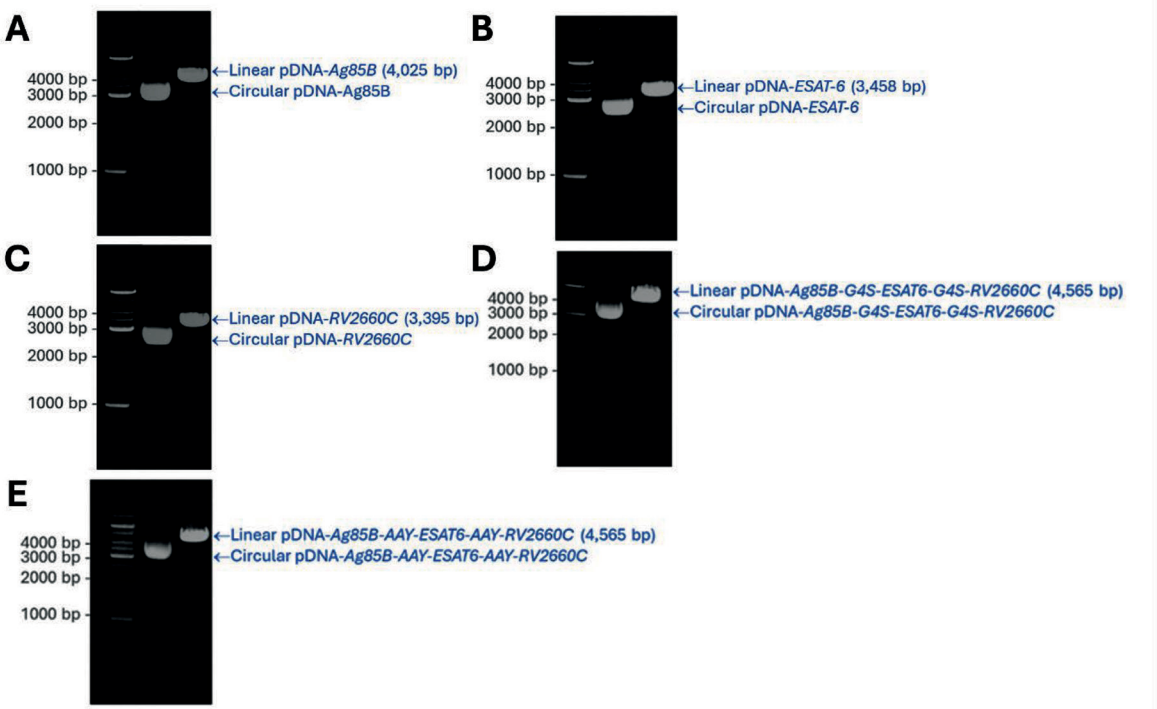

Figure 4 Agarose gel electrophoresis of linearized recombinant pDNA for the five MTB genes following restriction enzyme digestion: (A) *Ag85B*, (B) *ESAT-6*, (C) *Rv2660c*, (D) *Ag85B-G4S-ESAT-6-G4S-Rv2660c* fusion, and (E) *Ag85B-AAY-ESAT-6-AAY-Rv2660c* fusion.

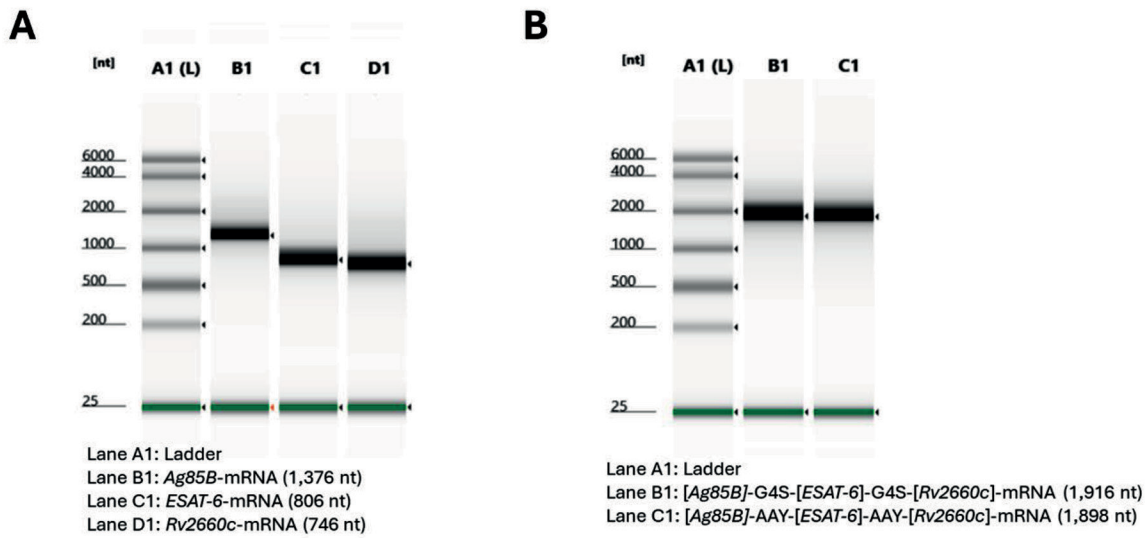

Figure 5 Analysis of synthesized mRNAs using the Agilent TapeStation Automated Electrophoresis System with the RNA ScreenTape kit, assessing the molecular size and quality of five MTB mRNA constructs. (A) *Ag85B*, *ESAT-6*, and *Rv2660c* individual mRNAs. (B) *Ag85B-G4S-ESAT-6-G4S-Rv2660c* fusion and *Ag85B-AAY-ESAT-6-AAY-Rv2660c* fusion mRNAs.

mRNA-LNPs Characterization

To evaluate the efficacy of LNP formulations in delivering mRNA, two systems, GenVoy-ILM™ and Moderna-like formulation, were initially compared using Fluc-mRNA as a control. GenVoy-ILM™ LNPs demonstrated encapsulation efficiency of 82.31%, significantly higher than Moderna's 68.55%, while achieving comparable average particle sizes (105.1±2.4 nm vs. 111.6±6.8 nm, respectively) and polydispersity index (PDI < 0.3) (Table 1). The zeta potential of both formulations was slightly negative (−8.1±1.4 mV for GenVoy-ILM™ and −5.9±1.2 mV for Moderna), supporting suspension stability. Based on this evaluation, GenVoy-ILM™ was selected for further studies due to its superior encapsulation efficiency.

Table 1 Physicochemical Properties of LNPs Formulations for Control and Target mRNA Constructs

mRNA	LNPs	RNA concentration (µg/mL)		Encapsulated mRNA (µg/mL)	Encapsulation efficiency (%EE)	Average Particle size (Z-Average[a]) (nm)	PDI[b]	Zeta potential (mV)
		Without Triton X-100	With 1 % Triton X-100					
Fluc-mRNA	GenVoy-ILM™	2.09	11.79	9.70	82.31	105.1± 2.4	0.199± 0.024	−8.1±1.4

Table 1 Physicochemical Properties of LNPs Formulations for Control and Target mRNA Constructs (continued)

mRNA	LNPs	RNA concentration (μg/mL)		Encapsulated mRNA (μg/mL)	Encapsulation efficiency (%EE)	Average Particle size (Z-Average[a]) (nm)	PDI[b]	Zeta potential (mV)
		Without Triton X-100	With 1 % Triton X-100					
Fluc-mRNA	mRNA-1273 (Moderna)	5.59	17.78	12.18	68.55	111.6± 6.8	0.128± 0.054	-5.9±1.2
Ag85B-G4S-ESAT-6-G4S-Rv2660c mRNA	GenVoy-ILM™	18.98	94.88	75.89	79.99	143.2± 2.3	0.099± 0.065	-2.9±0.4
Ag85B-AAY-ESAT-6-AAY-Rv2660c mRNA	GenVoy-ILM™	18.98	90.79	71.81	79.09	140.4± 4.1	0.089± 0.037	-22.7± 0.3

Note: [a] Z-average, Intensity-weighted mean hydrodynamic size

[b] PDI, polydispersity index. Data are expressed as mean±SD (n = 3)

GenVoy-ILM™ LNPs encapsulating *Ag85B-G4S-ESAT-6-G4S-Rv2660c* and *Ag85B-AAY-ESAT-6-AAY-Rv2660c* mRNAs yielded concentrations between 90.79 and 94.88 μg/mL, with both formulations achieving high encapsulation efficiency (%EE ~80%) (Table 1). *Ag85B-G4S-ESAT-6-G4S-Rv2660c* mRNA-LNPs had slightly larger average particle sizes (143.2±2.3 nm) compared to *Ag85B-AAY-ESAT-6-AAY-Rv2660c* mRNA-LNPs (140.4±4.1 nm), while both exhibited excellent size uniformity (PDI < 0.1) (Table1). Surface charge analysis revealed a more negative zeta potential for *Ag85B-AAY-ESAT-6-AAY-Rv2660c* mRNA-LNPs (-22.7±0.3 mV) compared to *Ag85B-G4S-ESAT-6-G4S-Rv2660c* mRNA-LNPs (-2.9±0.4 mV), suggesting higher colloidal stability for the former, as greater negative zeta potential is associated with improved stability in suspension.[17] These results confirmed the successful formulation and characterization of MTB-specific mRNA-LNPs, supporting their potential for further evaluation in preclinical applications.

In Vitro Protein Expression Studies

The functionality of the mRNA constructs was assessed through *in vitro* transfection of HEK293 cells using mRNA-LNP formulations containing either *Ag85B-G4S-ESAT-6-G4S-*

Rv2660c mRNA or *Ag85B-AAY-ESAT-6-AAY-Rv2660c* mRNA. Immunofluorescence assays demonstrated successful intracellular expression of the encoded fusion proteins, as indicated by distinct fluorescence signals corresponding to the target TB antigens. This observation further confirmed that the tPA secretory signal and MITD, as designed in the mRNA constructs, successfully facilitated the trafficking of the antigen to the cell surface. These signals resulted in effective antigen presentation, allowing the cells to be stained with specific antibodies against the TB antigens. In contrast, un-transfected HEK293 cells (without mRNA-LNP treatment) served as a negative control and showed no detectable fluorescence, confirming the specificity of the observed signals (Figure 6). These results demonstrated the successful delivery, translation, and trafficking of the mRNA constructs, enhancing antigen presentation at the cell surface.

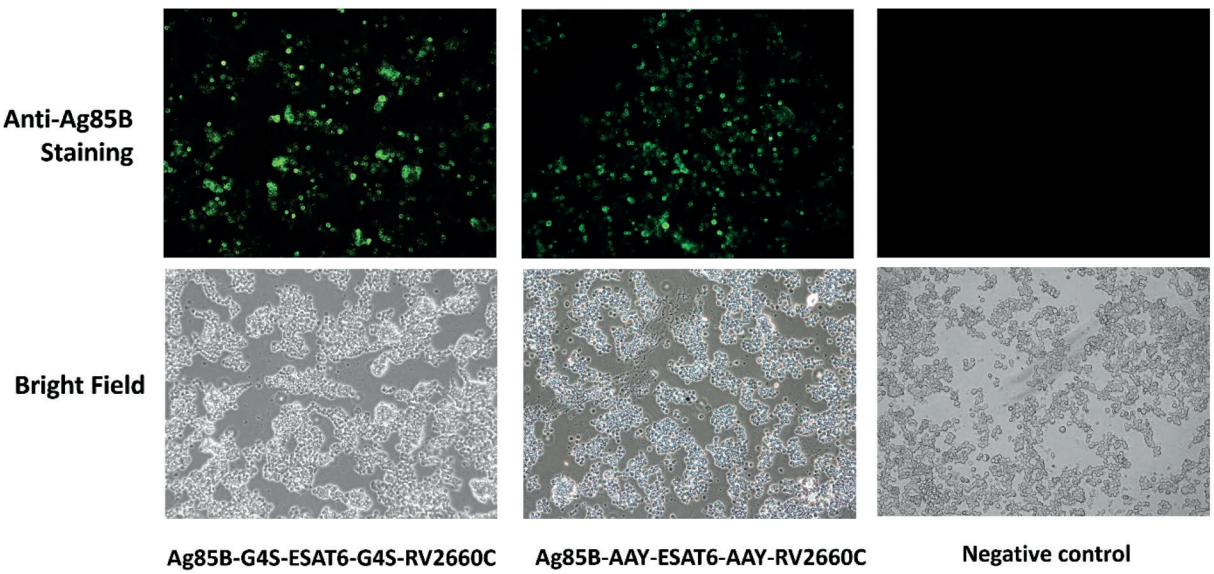

Figure 6. Immunofluorescence assay showing intracellular expression of TB antigens in HEK293 cells transfected with mRNA-LNP formulations (*Ag85B-G4S-ESAT-6-G4S-Rv2660c* mRNA and *Ag85B-AAY-ESAT-6-AAY-Rv2660c* mRNA). Green fluorescence indicated the expression of Ag85B in the transfected cells. Un-transfected HEK293 cells (negative control) exhibited no fluorescence, confirming the specificity of the observed signals. Images were captured at 10X magnification. Bright-field images show the overall morphology of the cells.

Discussion

This study successfully designed, synthesized, and encapsulated mRNA encoding MTB antigens into LNPs, demonstrating acceptable stability and efficient encapsulation, and target protein expression *in vitro*. These findings lay the groundwork for the future development of mRNA-based TB vaccines.

Five antigen mRNA constructs were designed, including individual antigens (*Ag85B, ESAT-6, and Rv2660c*) and fusion proteins (*Ag85B-G4S-ESAT-6-G4S-Rv2660c* and

Ag85B-AAY-ESAT-6-AAY-Rv2660c). These constructs were modified for efficient expression in human cells and structural stability with codon optimization parameters ensuring compatibility with the transcription and translation machinery.[12]

pDNA templates for *in vitro* transcription were successfully constructed, with homology confirmed across all nucleotide sequences. It is essential to verify the sequence, particularly in the region of the poly(A) tail, as its length and composition directly influence mRNA stability and translation efficiency.[18] To ensure the production of high-quality pDNA, the choice of *E. coli* strains and culture conditions played a crucial role in optimizing both yield and quality.[19]

mRNA synthesis was carried out using T7 RNA polymerase, with uridine triphosphate (UTP) replaced by N1-methylpseudouridine-5′-triphosphate and N7-methyl-3′-O-methylguanosine added to generate a cap 1 structure. These modifications significantly enhanced mRNA stability and translational efficiency while reducing innate immune activation.[20,21] The synthesis was performed on a small-scale using LiCl precipitation for purification. However, scaling up production will likely require advanced chromatography techniques to achieve higher purity and yield.[22] Our study confirmed that the synthesized mRNAs were intact and aligned with the expected sizes for all five genes.

The use of mRNA-loaded lipid nanoparticles (mRNA-LNPs) for vaccination and disease treatment has gained significant attention due to their ability to enhance mRNA stability, facilitate cellular uptake, and elicit robust immune responses. A critical factor in LNP formulation is achieving an optimal particle size, typically between 20 and 200 nm, to ensure stability in physiological fluids and effective tissue penetration.[20,23,24] In this study, we employed a microfluidic device for mRNA-LNP synthesis, enabling precise control over particle size and high reproducibility. The resulting LNPs carrying fusion antigen mRNAs had an average diameter of approximately 140 nm (Table 1) and an mRNA encapsulation efficiency of about 80%, regardless of the specific mRNA used. These findings were consistent with prior studies indicating that LNPs within this size range supported efficient delivery and immunogenicity.[20,23,24]

To ensure the safety and performance of mRNA-LNPs for future production, several additional analyses must be considered. These include physical characterization through visual inspection, evaluation of the lipid content after LNP formulation to ensure the desired ratio, and the determination of the optimal pH for the final formulation.[25,26] It is important to note that RNA integrity analysis is critical to confirm the quality of the encapsulated mRNA. Depending on the *in vitro* transcription conditions and subsequent purification steps, various byproducts, such as double-stranded RNA (dsRNA), abortive RNAs, and RNA-DNA hybrids, may be generated. If these byproducts are not adequately removed, they could be co-formulated with the full-length mRNA and potentially trigger unwanted immune responses in host cells by activating host pattern recognition receptors.[27] Additionally, endotoxin testing is essential to ensure the safety of the LNPs, as endotoxin contamination could lead to unwanted inflammatory responses.

Two LNP formulations, GenVoy-ILM™ and Moderna-like formulation, were evaluated for their mRNA encapsulation efficiency, particle size, and physicochemical properties. Both formulations showed similar performance; however, under our laboratory conditions, the GenVoy-ILM™ formulation achieved slightly higher encap-sulation efficiency, highlighting its potential as a promising candidate for vaccine development. Stability testing remains a crucial next step to assess long-term viability under different storage conditions, as temperature sensitivity is a known challenge for mRNA-based vaccines.[28]

This work built upon existing mRNA vaccine technologies by incorporating enhanced design features, such as fusion constructs and chemical modifications, to improve mRNA stability and translational efficiency. Several vaccine platforms, including traditional live attenuated vaccines,[3] protein subunit vaccines,[29] and viral vector vaccines[30] have been explored for TB. However, compared to these platforms, the mRNA approach offers significant advan-tages in terms of rapid production, scalability, and the ability to elicit robust humoral and cellular immune responses. Previous research has demonstrated that mRNA vaccines can effectively stimulate antigen-specific T-cell responses, a crucial factor for TB immunity.[31] Moreover, fusion protein constructs may provide broader antigenic coverage, potentially enhance immune responses when compared to single-antigen vaccines. By encoding multiple antigens within a single mRNA construct, this approach allowed for a more comprehensive immune response, potentially improving vaccine efficacy against diverse *M. tuberculosis* strains.

While this study demonstrated promising potential, further research is needed to advance these mRNA constructs toward clinical application. We have designed and characterized mRNA vaccine candidates for tuberculosis (TB) prevention. The preliminary data presented in this study outline the design of templates incor-porating antigens, including *Ag85B, ESAT-6*, and *Rv2660c*, used to create mRNA sequences encoding both individual and fusion antigens. These coding sequences were synthesized into mRNA via *in vitro* transcription and subsequently encapsulated into mRNA-LNPs. The resulting candidates exhibited results consistent with the original design. However, additional testing and further safety validation of the prototype vaccines are necessary, parti-cularly to identify any potential contaminants or issues arising from the product itself. These tests must align with international safety standards before progressing to the preclinical stage.

Key next steps include evaluating their immunogenicity and protective efficacy in preclinical models, optimizing lipid LNP formulations for greater stability under varied conditions, and addressing scalability and cost considerations. Continued efforts in these areas will be essential for translating this platform into a viable TB vaccine.

Conclusion

This study successfully designed and synthesized five mRNA constructs encoding MTB antigens: *Ag85B*, *ESAT-6*, *Rv2660c*, and two fusion constructs; *Ag85B-G4S-ESAT-6-G4S-Rv2660c* and *Ag85B-AAY-ESAT-6-AAY-Rv2660c*, all of which had the intact

structures and expected sizes. Due to their greater secondary structure stability compared to single-antigen constructs, only the two fusion constructs were encapsulated into LNPs. Characterization of the mRNA-LNPs revealed that *Ag85B-AAY-ESAT-6-AAY-Rv2660c* mRNA-LNPs exhibited higher colloidal stability. Nevertheless, both mRNA-LNP formulations effectively delivered mRNA and facilitated robust protein expression in human cell lines. These findings highlight the potential of these mRNA constructs as promising candidates for tuberculosis vaccine development.

Acknowledgment

We gratefully acknowledge the Thailand Science Research and Innovation (TSRI) for their funding support of this research project through the National Vaccine Institute (NVI), Thailand, as Project No. 2566.1/22.

References

1. World Heatlh Organization. Global tuberculosis report 2024. Geneva: World Heatlh Organization; 2024.
2. Kiazyk S, Ball TB. Latent tuberculosis infection: an overview. Can Commun Dis Rep 2017; 43(3-4): 62-6.
3. Setiabudiawan TP, Reurink RK, Hill PC, Netea MG, van Crevel R, Koeken V. Protection against tuberculosis by Bacillus Calmette-Guérin (BCG) vaccination: a historical perspective. Med 2022; 3(1): 6-24.
4. กรมควบคุมโรค กระทรวงสาธารณสุข. แผนปฏิบัติการระดับชาติ ด้านการต่อต้านวัณโรค ระยะที่ 2 (พ.ศ. 2566 - 2570). นนทบุรี: กองวัณโรค กรมควบคุมโรค กระทรวงสาธารณสุข; 2566.
5. Liu W, Xu Y, Yan J, Shen H, Yang E, Wang H. Ag85B synergizes with ESAT-6 to induce efficient and long-term immunity of C57BL/6 mice primed with recombinant Bacille Calmette-Guerin. Exp Ther Med 2017; 13(1): 208-14.
6. van Dissel JT, Arend SM, Prins C, Bang P, Tingskov PN, Lingnau K, et al. Ag85B-ESAT-6 adjuvanted with IC31 promotes strong and long-lived *Mycobacterium tuberculosis* specific T cell responses in naïve human volunteers. Vaccine 2010; 28(20): 3571-81.
7. Nemes E, Geldenhuys H, Rozot V, Rutkowski KT, Ratangee F, Bilek N, et al. Prevention of *M. tuberculosis* infection with H4:IC31 vaccine or BCG revaccination. N Engl J Med 2018; 379(2): 138-49.
8. Aagaard C, Hoang T, Dietrich J, Cardona PJ, Izzo A, Dolganov G, et al. A multistage tuberculosis vaccine that confers efficient protection before and after exposure. Nat Med 2011; 17(2): 189-94.
9. Bekker LG, Dintwe O, Fiore-Gartland A, Middelkoop K, Hutter J, Williams A, et al. A phase 1b randomized study of the safety and immunological responses to vaccination with H4:IC31, H56:IC31, and BCG revaccination in *Mycobacterium tuberculosis*-uninfected adolescents in Cape Town, South Africa. EClinicalMedicine 2020; 21: 100313. (11 pages).

10. Jenum S, Tonby K, Rueegg CS, Rühwald M, Kristiansen MP, Bang P, et al. A Phase I/II randomized trial of H56:IC31 vaccination and adjunctive cyclooxygenase-2-inhibitor treatment in tuberculosis patients. Nat Commun 2021; 12(1): 6774. (13 pages).
11. Xue T, Stavropoulos E, Yang M, Ragno S, Vordermeier M, Chambers M, et al. RNA encoding the MPT83 antigen induces protective immune responses against *Mycobacterium tuberculosis* infection. Infect Immun 2004; 72(11): 6324-9.
12. Al Tbeishat H. Novel In Silico mRNA vaccine design exploiting proteins of *M. tuberculosis* that modulates host immune responses by inducing epigenetic modifications. Sci Rep 2022; 12(1): 4645. (19 pages).
13. Vostrosablin N, Lim S, Gopal P, Brazdilova K, Parajuli S, Wei X, et al. mRNAid, an open-source platform for therapeutic mRNA design and optimization strategies. NAR Genom Bioinform 2024; 6(1): lqae028. (9 pages).
14. McKenzie RE, Minnell JJ, Ganley M, Painter GF, Draper SL. mRNA synthesis and encapsulation in ionizable lipid nanoparticles. Curr Protoc 2023; 3(9): e898. (47 pages).
15. Gambaro R, Rivero Berti I, Limeres MJ, Huck-Iriart C, Svensson M, Fraude S, et al. Optimizing mRNA-loaded lipid nanoparticles as a potential tool for protein-replacement therapy. Pharmaceutics 2024; 16(6): 771. (23 pages).
16. Mathews DH, Sabina J, Zuker M, Turner DH. Expanded sequence dependence of thermodynamic parameters improves prediction of RNA secondary structure. J Mol Biol 1999; 288(5): 911-40.
17. Pochapski DJ, Carvalho Dos Santos C, Leite GW, Pulcinelli SH, Santilli CV. Zeta potential and colloidal stability predictions for inorganic nanoparticle dispersions: effects of experimental conditions and electrokinetic models on the interpretation of results. Langmuir 2021; 37(45): 13379-89.
18. Gergen J, Petsch B. mRNA-based vaccines and mode of action. Curr Top Microbiol Immunol 2022; 440: 1-30.
19. Al-Allaf FA, Tolmachov OE, Zambetti LP, Tchetchelnitski V, Mehmet H. Remarkable stability of an instability-prone lentiviral vector plasmid in Escherichia coli Stbl3. 3 Biotech 2013; 3(1): 61-70.
20. Chaudhary N, Weissman D, Whitehead KA. mRNA vaccines for infectious diseases: principles, delivery and clinical translation. Nat Rev Drug Discov 2021; 20(11): 817-38.
21. Karikó K, Muramatsu H, Welsh FA, Ludwig J, Kato H, Akira S, et al. Incorporation of pseudouridine into mRNA yields superior nonimmunogenic vector with increased translational capacity and biological stability. Mol Ther 2008; 16(11): 1833-40.
22. Feng X, Su Z, Cheng Y, Ma G, Zhang S. Messenger RNA chromatographic purification: advances and challenges. J Chromatogr A 2023; 1707: 464321. (14 pages).
23. Shi R, Liu X, Wang Y, Pan M, Wang S, Shi L, et al. Long-term stability and immunogenicity of lipid nanoparticle COVID-19 mRNA vaccine is affected by particle size. Hum Vaccin Immunother 2024; 20(1): 2342592. (11 pages).
24. Oberli MA, Reichmuth AM, Dorkin JR, Mitchell MJ, Fenton OS, Jaklenec A, et al. Lipid nanoparticle assisted mRNA delivery for potent

cancer immunotherapy. Nano Lett 2017; 17(3): 1326-35.

25. Wu K, Xu F, Dai Y, Jin S, Zheng A, Zhang N, et al. Characterization of mRNA-LNP structural features and mechanisms for enhanced mRNA vaccine immunogenicity. J Control Release 2024; 376: 1288-99.
26. Ma Y, VanKeulen-Miller R, Fenton OS. mRNA lipid nanoparticle formulation, characterization and evaluation. Nat Protoc. [online]. 2025; [cited 2025 Mar 12]. Available from: URL: https://doi.org/10.1038/s41596-024-01134-4.
27. Lenk R, Kleindienst W, Szabó GT, Baiersdörfer M, Boros G, Keller JM, et al. Understanding the impact of in vitro transcription byproducts and contaminants. Front Mol Biosci 2024; 11: 1426129. (16 pages).
28. Rosa SS, Prazeres DMF, Azevedo AM, Marques MPC. mRNA vaccines manufacturing: challenges and bottlenecks. Vaccine 2021; 39(16): 2190-200.
29. Zhang Y, Xu JC, Hu ZD, Fan XY. Advances in protein subunit vaccines against tuberculosis. Front Immunol 2023; 14: 1238586. (14 pages).
30. Hu Z, Lu SH, Lowrie DB, Fan XY. Research advances for virus-vectored tuberculosis vaccines and latest findings on tuberculosis vaccine development. Front Immunol 2022; 13: 895020. (16 pages).
31. Lukeman H, Al-Wassiti H, Fabb SA, Lim L, Wang T, Britton WJ, et al. An LNP-mRNA vaccine modulates innate cell trafficking and promotes polyfunctional Th1 CD4+ T cell responses to enhance BCG-induced protective immunity against *Mycobacterium tuberculosis*. eBioMedicine 2025; 113: 105599. (16 pages).

การออกแบบและการวิเคราะห์คุณลักษณะเบื้องต้นของ *Ag85B-ESAT-6-Rv2660c* mRNA-Lipid Nanoparticles เพื่อการพัฒนาวัคซีนป้องกันวัณโรค

ปนัดดา เทพอัคศร อภิชัย ประชาสุภาพ กชรัตน์ จงปิติทรัพย์ พันธ์ธิดา ตรียวง ศิรวิทย์ เวทโอสถ อณิชา เลื่องชัยเชวง รุจิราพร พิทักษ์สาลี และ ภาณุพันธ์ ปัญญาใจ
สถาบันชีววิทยาศาสตร์ทางการแพทย์ กรมวิทยาศาสตร์การแพทย์ นนทบุรี 11000

บทคัดย่อ วัณโรคเป็นปัญหาสาธารณสุขที่สำคัญในหลายประเทศทั่วโลก ปัจจุบันประเทศไทยถูกจัดให้เป็นกลุ่มประเทศที่มีภาระวัณโรคสูงของโลก (High Burden Country Lists) โดยมีอุบัติการณ์ผู้ป่วยวัณโรคสูงกว่าค่าเฉลี่ยของประชากรโลก วัคซีนบีซีจี (Bacillus Calmette–Guérin) เป็นวัคซีนเพียงชนิดเดียวที่ใช้ป้องกันวัณโรคชนิดรุนแรงในเด็ก แต่กลับพบว่ามีประสิทธิภาพในการป้องกันวัณโรคลดลงในผู้ใหญ่ ดังนั้นการวิจัยและพัฒนาวัคซีนวัณโรคชนิดใหม่ ๆ จึงมีความสำคัญเพื่อให้บรรลุเป้าหมายการยุติวัณโรคและการพัฒนาที่ยั่งยืนของประเทศไทย การศึกษานี้มุ่งเน้นการออกแบบและการวิเคราะห์คุณลักษณะของ mRNA สำหรับพัฒนาเป็นวัคซีนป้องกันวัณโรคโดยใช้แอนติเจนหลักสามชนิด ได้แก่ Ag85B, ESAT-6 และ Rv2660c ซึ่งมีบทบาทในระยะต่าง ๆ ของการติดเชื้อ *Mycobacterium tuberculosis* (MTB) ได้ดำเนินการออกแบบและสังเคราะห์ mRNA ทั้งหมด 5 ชนิด ในหลอดทดลอง ประกอบด้วย mRNA ของแอนติเจนเดี่ยว 3 รูปแบบ และรูปแบบ fusion ซึ่งประกอบด้วยแอนติเจนทั้งสามชนิด จำนวน 2 รูปแบบ โดยพบว่ารูปแบบ fusion ของ *Ag85B-G4S-ESAT-6-G4S-Rv2660c* mRNA และ *Ag85B-AAY-ESAT-6-AAY-Rv2660c* mRNA มีความเสถียรสูงกว่ารูปแบบแอนติเจนเดี่ยว และเมื่อนำ mRNA รูปแบบ fusion มาห่อหุ้มในอนุภาคไขมันนาโน (mRNA-LNPs) พบว่ามีประสิทธิภาพการห่อหุ้ม (%Encapsulation Efficiency) สูง โดยมีขนาดอนุภาคสม่ำเสมอเฉลี่ยประมาณ 140 นาโนเมตร และมีความคงตัวสูง นอกจากนี้เมื่อนำส่ง mRNA-LNPs เข้าสู่เซลล์ HEK293 พบว่ามีการแสดงออกของโปรตีนรูปแบบ fusion ซึ่งยืนยันโดยการย้อมด้วยแอนติบอดีจำเพาะต่อแอนติเจนของเชื้อวัณโรค ดังนั้น modified *Ag85B-ESAT-6-Rv2660c* mRNA ที่สร้างขึ้นจึงมีคุณลักษณะเหมาะสม และมีศักยภาพในการพัฒนาเป็นวัคซีนป้องกันวัณโรคต่อไป

คำสำคัญ: วัณโรค, วัคซีน mRNA, *Ag85B-ESAT-6-Rv2660c*, อนุภาคไขมันนาโน